

1 **Supplemental materials:**

2  
3 **Methods**

4 **Synthesis of PIP compounds**

5 The reagents and solvents were purchased from standard suppliers and used without  
6 further purification. HPLC analysis of the compounds was performed on a Jasco Engineering  
7 PU-2089 plus series system using a COSMOSIL 150×4.6 mm 5C<sub>18</sub>-MS-II Packed Column  
8 (Nacalai Tesque, Inc.) in 0.1% trifluoroacetic acid in water with acetonitrile as the eluent at  
9 a flow rate of 1.0 mL/min and a linear gradient elution of 0–100% acetonitrile in 40 min with  
10 detection at 254 nm. The collected fractions were analyzed using MALDI-TOF MS  
11 microflex-KS II (Bruker).

12 CWG-cPIP and CWG-hPIP were synthesized as reported previously (37) and purified  
13 using the CombiFlash Rf RFJ model with RediSep Rf 4.3 g C18 reverse-phase column  
14 (Teledyne Isco, Inc.).

15 To obtain FITC-labeled CWG-cPIP, Cbz-protected cPIP, cyclo-(-ImPyβImPy-(R)<sup>α</sup>-  
16 NH<sub>2</sub>-γ-ImPyβImPy-(R)<sup>α</sup>-NH<sup>Cbz</sup>-γ-), was synthesized following procedures similar to those  
17 described previously (36). The crude sample was dissolved in *N, N*-dimethylformamide  
18 (DMF), and Fmoc-mini-PEG<sup>TM</sup> (1.5 equiv.; Peptides International, Inc.), pentafluorophenyl  
19 diphenylphosphinate (1.5 equiv.) and diisopropylethylamine (DIEA, 3 equiv.) were added to  
20 it, and the mixture was then stirred for 4 h at room temperature. The mixture was dropped  
21 into Et<sub>2</sub>O and subjected to centrifugation, following which Et<sub>2</sub>O was removed and the pellet  
22 was dried in vacuo. The Fmoc protecting group was removed by 20% piperidine/DMF  
23 treatment for 30 min at room temperature. The mixture was precipitated in Et<sub>2</sub>O and the

24 resulting powder was dried in vacuo. The pellet was dissolved in DMF with fluorescein 5-  
25 isothiocyanate (2 equiv.) and DIEA (6 equiv.), and the mixture was stirred for 2 h at room  
26 temperature. After the workup, the Cbz protecting group was removed using  
27 trifluoromethanesulfonic acid/trifluoroacetic acid (1:10) treatment for 4 min at room  
28 temperature. Workup with Et<sub>2</sub>O gave a crude powder of cyclo-(-ImPyβImPy-(R)<sup>α-NH<sub>2</sub></sup>-γ-  
29 ImPyβImPy-(R)<sup>α-NH-miniPEG-FITC</sup>-γ-). After purification, 5.4 mg of the sample was obtained (2.9  
30 μmol, 9% yield for 18 steps). Analytical HPLC: t<sub>R</sub>=17.7 min. MALDI-TOF MS: *m/z* calcd.  
31 for C<sub>85</sub>H<sub>93</sub>N<sub>28</sub>O<sub>20</sub>S<sup>+</sup> [M+H]<sup>+</sup> 1857.68, found; 1857.74. The HPLC and MALDI-TOF MS  
32 spectra of FITC-labeled CWG-cPIP are shown in Supplementary Figure 2.

33

#### 34 **Structural model of CWG-cPIP binding to DNA**

35 Molecular modeling studies were performed with Discovery Studio (BIOVIA) using  
36 the charmm27 force field. The initial PIP structure was built based on previous crystal  
37 structures (PDB ID: 3I5L) and manually inserted into the minor groove of the B-DNA  
38 sequence 5'-GCAGCAGCAGC-3'/3'-CGTCGTCGTCG-5' constructed using the builder  
39 module. The complex was solvated in cubic water with 50 mM NaCl and pre-minimized to  
40 maintain the interaction distance of hydrogen bonds between the polyamide moiety and DNA  
41 base pairs. Then, A and T in the sequence were replaced with each DNA base to obtain the  
42 B-DNA sequence (5'-GCNGCNGCNGC-3'/3'-CGNCGNCGNCG-5', N = A, T, G, C). The  
43 entire structure was finally minimized to the stage where the root-mean-square was less than  
44 0.001 kcal/mol·Å using the conjugate gradient algorithm with no constraint.

45

## 46 **Melting temperature $T_m$ assay**

47 DNA and RNA oligomers were purchased from Fasmac and Hokkaido System  
48 Science, respectively: 1) d(CAG/CTG) (5'-CGAGCAGCACG-3'/5'-CGTGCTGCTCG-3');  
49 2) d(CGG/CCG) (5'-CGGGCGGCGCG-3'/5'-CGCGCCGCCCG-3'); 3) AT rich (5'-  
50 CGATTATTACG-3'/5'-CGTAATAATCG-3') 4) GC rich (5'-CGGCGCCGCCG-3'/5'-  
51 CGGCGGCGCCG-3'); 5) 5'-d(CAG)<sub>10</sub> repeat-3'; 6) 5'-d(CTG)<sub>10</sub> repeat-3'; 7) 5'-d(CGG)<sub>10</sub>  
52 repeat-3'; 8) 5'-d(CCG)<sub>10</sub> repeat-3'; 9) 5'-r(CAG)<sub>10</sub> repeat-3'; 10) 5'-r(CUG)<sub>10</sub> repeat-3'. The  
53 analytical buffer used for the  $T_m$  assay was an aqueous solution of NaCl (2.5 mM) and Tris-  
54 HCl (10 mM) at pH 7.5 containing 0.375% DMSO. The concentrations of double-stranded  
55 DNA, mismatched hairpin DNA, and mismatched hairpin RNA were 2.5  $\mu$ M. The  
56 concentration of polyamides was 3.75  $\mu$ M (1.5 equiv.). Before the analysis, the samples were  
57 annealed from 95°C to 20°C at a rate of 1.0°C/min, and the absorbance at 260 nm was  
58 recorded from 20°C to 95°C at a rate of 1.0°C/min using a spectrophotometer (V-750;  
59 JASCO, Inc.) with a thermocontrolled cell changer (PAC-743R; JASCO, Inc.) and a thermal  
60 circulator (CTU-100; JASCO, Inc.). The  $T_m$  values shown in Figure 1B are the averages of  
61 all data. The calculated  $T_m$  and  $\Delta T_m$  values are presented in Supplementary Table 1.

62

## 63 **Plasmid constructs**

64 For transcription arrest assay, a random sequence of 189 base pairs with (CTG)<sub>10</sub>  
65 repeats at the N-terminus or a (CTG)<sub>73</sub> repeat sequence was subcloned into pcDNA3.1(+),  
66 termed pT7(CTG)<sub>10</sub> or pT7(CTG)<sub>73</sub>, respectively. The (CTG)<sub>73</sub> sequence was obtained from  
67 plasmid pAAV-CTG700x (#63087; Addgene). Random DNA sequence was synthesized

68 commercially by Eurofins Genomics. To evaluate the production of CWG repeat RNAs in  
69 cells, we generated a dual promoter vector pFC-EF1-MCS-pA-PGK-EGFP using PhiC31  
70 vector (FC551A-1; System Biosciences, LLC) as a backbone. For HaloTag-CTG repeat  
71 mRNA expression plasmid, a subcloned fragment with (CTG)<sub>10</sub>, (CTG)<sub>180</sub>, or (CTG)<sub>700</sub> repeat  
72 sequence in the 3'-UTR of HaloTag was inserted into the MCS of pFC-EF1-MCS-pA-PGK-  
73 EGFP vector, termed CUG10, CUG180 or CUG700, respectively. These CTG repeat  
74 sequences were obtained from plasmid pAAV-CTG700x (#63087; Addgene). For HaloTag-  
75 CAG repeat mRNA expression plasmid, a subcloned fragment of (CAG)<sub>23</sub> or (CAG)<sub>74</sub> repeat  
76 sequence within exon 1 of the *HTT* gene was inserted into the MCS of pFC-EF1-MCS-pA-  
77 PGK-EGFP vector. These CAG repeat sequences were obtained from plasmid pEGFP-Q23  
78 and pEGFP-Q74 (#40261 and #40262, respectively; Addgene). For EGFP-CTG repeat  
79 mRNA expression plasmid, a subcloned fragment with (CTG)<sub>10</sub> or (CTG)<sub>700</sub> repeat sequences  
80 in the 3'-UTR of *Egfp* were inserted into the MCS of pCAG-Neo vector (Wako Pure  
81 Chemical). For EGFP-CTG repeat mRNA expression AAV vector plasmid, a fragment with  
82 (CTG)<sub>10</sub> or (CTG)<sub>300</sub> repeat sequence in the 3'-UTR of *Egfp* was subcloned into plasmid  
83 pAAV-CTG700x (#63087; Addgene), termed pAAV-CUG10, pAAV-CUG300, respectively.  
84 For EGFP-CAG repeat (EGFP-polyQ) expression AAV vector plasmid, a fragment of *Egfp*  
85 with (CAG)<sub>23</sub> or (CAG)<sub>74</sub> repeat sequence at the C-terminus was subcloned into plasmid  
86 pAAV-CTG700 (#63087; Addgene), termed pAAV-Q23 or pAAV-Q74, respectively.

87

## 88 **Transcription arrest assay**

89           The pT7(CTG)<sub>10</sub> and pT7(CTG)<sub>73</sub> plasmids were linearized using EcoRI restriction  
90 enzyme and purified using the Wizard SV Gel and PCR Clean-Up System (Promega).  
91 Transcription arrest assays were performed using HiScribe T7 high-yield RNA synthesis kit  
92 (New England Biolabs) with 0.5% DMSO (vehicle) or CWG-cPIP (1.25, 2.5, or 3.75  $\mu$ M),  
93 and 200 ng of the linearized plasmid was obtained, which produces a 321-base RNA under  
94 the T7 promoter. After transcription for 10 min at 37°C, DNase I was added according to the  
95 manufacturer's instructions. Transcription products were analyzed by urea-denaturing  
96 polyacrylamide gel electrophoresis on 7% gels containing 7 M urea at 200 V for 120 min.  
97 Before loading, samples were heated for 4 min at 90°C with RNA Loading Dye (New  
98 England Biolabs), and then immediately cooled on ice for a few minutes. After the  
99 electrophoresis, the gels were stained with SYBR Gold (Invitrogen) for 20 min and visualized  
100 using Typhoon Trio equipment (GE Healthcare).

101

## 102 **Cell culture**

103           Cell cultures were established according to previously described methods (87). The  
104 Neuro-2a mouse neuroblastoma cell line CCL-131 was authenticated by the provider using  
105 short tandem repeat profiling (American Type Culture Collection) and was grown in DMEM  
106 (Sigma-Aldrich) supplemented with 10% FBS (Gibco) and 1 $\times$  penicillin/streptomycin  
107 (Gibco) in a 5% CO<sub>2</sub> incubator at 37°C. Transfection was performed using the Lipofectamine  
108 2000 Transfection Reagent (Invitrogen) according to the manufacturer's protocol. For the  
109 primary culture of neurons, cortical tissue was dissected and dispersed from the mice on  
110 embryonic day 18. Cells were seeded on coverslips coated with poly-L-lysine in MEM

111 (Thermo Fisher Scientific) supplemented with 10% FBS, 0.6% glucose (Wako Pure  
112 Chemical), and 1 mM pyruvate (Sigma-Aldrich). After cell attachment, the cells were  
113 cultured in Neuron Culture Medium (Wako Pure Chemical) in a 5% CO<sub>2</sub> incubator at 37°C.  
114 Cultured neurons were transfected with plasmids using an electroporator (NEPA21; Nepa  
115 Gene) on day 0 in vitro (DIV0), and subjected to biochemical experiments on DIV14. Human  
116 fibroblasts [GM23966 (healthy control) and GM03132 (DM1 with (CTG)<sub>1700</sub> repeats) for  
117 CTG repeats; GM23974 (healthy control) and GM09197 (HD with (CAG)<sub>180</sub> repeats) for  
118 CAG repeats; Coriell Institute for Medical Research] were seeded onto gelatin-coated culture  
119 plates (20,000–40,000 cells/well in 12-well plates) and cultured in DMEM supplemented  
120 with 10% FBS and 1× penicillin-streptomycin for 24 h. The cells were then transferred to a  
121 neuronal induction medium containing equal volumes of DMEM/F12 and Neurobasal  
122 Medium supplemented with 0.5% N-2, 1% B-27 (all from Gibco), and 100 μM cAMP  
123 (Sigma-Aldrich) with small molecules (0.5 mM valproic acid, 3 μM CHIR99021, 1 μM  
124 Repsox, 10 μM forskolin, 10 μM SP600125, 5 μM GO6983, 5 μM Y-27632, 20 μM ISX-9,  
125 and 2 μM I-BET151; Sigma-Aldrich) according to previously described methods (88, 89).  
126 Three days after treatment, we confirmed that a significant fraction (approximately 90%) of  
127 cells derived from healthy controls and DM1 patients exhibited typical neuronal morphology  
128 and expressed the neuronal marker Tuj1. Because iNeurons were not efficiently obtained  
129 from HD patient-derived fibroblasts used in this study (approximately less than 1%), the cells  
130 from HD patients and the corresponding healthy controls were used as fibroblasts for the  
131 following experiments.

132

133 **Cell viability assay**

134 Cell viability was measured using the Cell Counting Kit-8 (Dojindo Molecular  
135 Technologies, Inc.), according to the manufacturer's instructions. Neuro-2a cells were  
136 cultured in 96-well plates (2,000 cells/well) at 37°C for 24 h and treated with 0.1% DMSO  
137 (vehicle) or CWG-cPIP at different concentrations (0.1, 0.3, 1, 3, 10, or 30 μM). After 47 h,  
138 CCK-8 solution was added to each well, followed by incubation for 1 hour at 37°C.  
139 Absorbance at 450 nm was measured using a plate reader (Multiskan FC; Thermo Fisher  
140 Scientific). The viability of CWG-cPIP-treated cells was expressed as a percentage of that of  
141 the vehicle-treated cells.

142

143 **RT-qPCR analysis**

144 Sample preparation for RT-qPCR from Neuro-2a cells was performed using the  
145 SuperPrep II Cell Lysis & RT Kit qPCR (TOYOBO). Sample preparation for RT-qPCR from  
146 primary cultured neurons was performed using an RNeasy Mini Kit (QIAGEN) and  
147 PrimeScript RT Master Mix (Takara Bio, Inc.). RT-qPCR was performed using the KOD  
148 SYBR qPCR Mix (TOYOBO) on a CFX Connect Real-Time PCR System (Bio-Rad  
149 Laboratories, Inc.). Gene expression was assessed using differences in the normalized Ct  
150 (cycle threshold;  $\Delta\Delta Ct$ ) method after normalization to *Egfp* expression. Fold-changes were  
151 calculated using the  $2^{-\Delta\Delta Ct}$  method. The following primers were used for RT-qPCR: *Egfp*  
152 (forward, 5'-CACATGAAGCAGCAGACTTC-3'; reverse, 5'-  
153 TTCAGCTCGATGCGGTTTAC-3'), HaloTag (forward, 5'-  
154 AGAATACATGGACTGGCTGC-3'; reverse, 5'-TCTTGCAGCAGATTCAGACC-3'),

155 mouse *Htt* (forward, 5'-CCCCATTCATTGCCTTGCTG-3'; reverse, 5'-  
156 CTTGAGCGACTCGAAAGCCT-3'), human *HTT* (forward, 5'-  
157 AGGTTCGCTTTTACCTGCGG-3'; reverse, 5'-CATCAGCTTTTCCAGGGTCG-3'), and  
158 *Gapdh* (forward, 5'-AACTTTGGCATTGTGGAAGG-3'; reverse, 5'-  
159 ACACATTGGGGGTAGGAACA-3').

160

## 161 **Antibodies**

162 The following primary antibodies were used: anti-GFP (1:1000; ab290, Abcam), anti-  
163 GFP (1:500; clone 9F9.F9, ab1218, Abcam), anti-NeuN (1:2000; ABN90, Millipore), anti-  
164 cleaved caspase-3 (1:500; ab2302, Abcam), anti-Tuj1 (1:2000, 802001, BioLegend), anti-  
165 MBNL1 (1:500; ab45899, Abcam), anti- $\beta$ -actin (1:1000; ab8227, Abcam), anti-Huntingtin  
166 (1:100; clone 3E10, sc-47757, Santa Cruz), anti-polyglutamine-expansion diseases marker  
167 (1:1000; clone 1C2, MAB1574, Millipore), anti-Huntingtin (1:500; clone MW8, MW8,  
168 DSHB deposited by Dr. P. H. Patterson), and anti-K63-specific ubiquitin (1:500; clone Apu3,  
169 05-1308, Millipore). The following secondary antibodies were used: HRP-conjugated anti-  
170 mouse IgG antibody (1:5000; 1031-05, SouthernBiotech), and HRP-conjugated anti-rabbit  
171 IgG antibody (1:5000; 4050-05, SouthernBiotech), Alexa 488-conjugated donkey anti-rabbit  
172 (1:500; A-21206, Invitrogen), Alexa 594-conjugated donkey anti-rabbit (1:500; A-21207,  
173 Invitrogen), Alexa 488-conjugated donkey anti-mouse (1:500; A-21202, Invitrogen), Alexa  
174 594-conjugated donkey anti-mouse (1:500; A-21203, Invitrogen), and Alexa 594-conjugated  
175 donkey anti-guinea pig (1:500; 706-585-148, Jackson ImmunoResearch Laboratories).

176

177 **Histology**

178 Brain tissues were fixed in 4% paraformaldehyde in PBS, sliced coronally at a  
179 thickness of 50  $\mu\text{m}$ , and then incubated with 0.1% cresyl violet acetate (pH 4.8) for 10 min  
180 at 37°C. After differentiation with 95% ethanol and 0.1% acetate, the sections were  
181 dehydrated through a graded ethanol series, cleared with xylene, and mounted with Entellan  
182 new (Sigma-Aldrich). The sections were analyzed and imaged using a confocal laser  
183 scanning microscope (TCS SP8; Leica Microsystems).

184

185 **Immunocytochemistry and immunohistochemistry**

186 Immunocytochemistry and immunohistochemistry were performed as previously  
187 described (87). Briefly, brain slices and cells were fixed in 4% paraformaldehyde in PBS and  
188 then treated with PBS containing 0.3% Triton X-100 for 10 min. To detect polyQ-positive  
189 aggregates, immunofluorescence was performed as previously described (90). Briefly, the  
190 slices were treated with 88% formic acid for 10 min at room temperature and washed with  
191 running water, and then with PBS. The sections were then treated with PBS containing 0.4%  
192 Triton X-100 thrice for 10, 30, and 10 min. The samples were incubated overnight at 4°C  
193 with primary antibodies, washed in PBS, and incubated with fluorophore-labeled secondary  
194 antibodies. Nuclei were counterstained with DAPI (Thermo Fisher Scientific). The samples  
195 were mounted using VECTASHIELD (Vector Laboratories, Inc.), and fluorescence images  
196 were analyzed using a confocal laser scanning microscope (LSM900; Carl Zeiss).

197

198 **FISH**

199 Fixed brain slices and cells were washed three times with diethylpyrocarbonate-  
200 treated PBS (DEPC-PBS) for 10 min each and then incubated with 0.3% Triton X-100 in  
201 DEPC-PBS for 10 min. After several washes, the slices and cells were prehybridized with  
202 40% formamide in 2× SSC (300 mM NaCl and 30 mM sodium citrate) for 10 min at room  
203 temperature, followed by incubation with a 1 nM Cy5-(CAG)<sub>10</sub> DNA probe in hybridization  
204 solution (2× SSC, 40% formamide, 10% dextran sulfate, 2 mM ribonucleoside-vanadyl  
205 complex, 0.5 mg/mL yeast transfer RNA) at 37°C overnight. After hybridization, the samples  
206 were washed with 40% formamide in 2× SSC and then with 1× SSC each for 15 min at 37°C.  
207 The samples were rinsed with DEPC-PBS and subjected to immunofluorescence procedure.

208

### 209 **Western blotting**

210 Immunoblotting was performed as described previously (87). Briefly, the cells were  
211 homogenized in RIPA buffer containing protease and phosphatase inhibitor cocktails  
212 (Nacalai Tesque, Inc.). Equivalent amounts of protein were subjected to SDS-PAGE.  
213 Separated proteins were transferred to an Immobilon PVDF membrane. The membrane was  
214 blocked with Tris-buffered saline (50 mM Tris-HCl, pH 7.5 and 150 mM NaCl) with 0.1%  
215 Tween 20 (TBST) solution containing 5% fat-free milk powder for 1 h at room temperature,  
216 and then incubated overnight at 4°C with primary antibodies. The membrane was then  
217 washed with TBST and incubated with HRP-conjugated secondary antibodies diluted in  
218 TBST for 1 h at room temperature. Blots were developed using an HRP substrate (32132;  
219 Thermo Fisher Scientific), and the immunoreactive bands were visualized using a  
220 chemiluminescence imaging system (FUSION SOLO; Vilber Bio Imaging).

221

## 222 **RNA-Seq analysis**

223 Total RNA was extracted from the mouse hippocampus using an RNeasy Mini Kit  
224 (QIAGEN). DNA libraries were prepared using NEBNext Ultra II Directional RNA Library  
225 Prep Kit for Illumina and sequenced by NextSeq 500 (Illumina, Inc.) to obtain single-end  
226 reads (75 nt) for off-target analysis and paired-end reads (150 nt) for splicing analysis,  
227 respectively. For off-target analysis, the extracted RNA was mixed with ERCC RNA Spike-  
228 In Mix (Invitrogen) containing 92 polyadenylated transcripts with concentration spanning  
229  $10^6$ -fold range prior to library preparation. After base calling, the sequences were  
230 demultiplexed and FASTQ files were generated using the Generate FASTQ Analysis Module  
231 in the Local Run Manager (Illumina, Inc.). The adapter sequence and low-quality ends were  
232 trimmed using the Trim Galore! (version 0.6.6). The RSEM package (version 1.3.3) in  
233 conjunction with the STAR aligner (version 2.7.9a) was used to align sequences with the  
234 mouse reference genome (UCSC GRCm38/mm10) and determine gene expression. Gene  
235 expression for each sample was further processed using DESeq2 (version 1.36.0) and  
236 expressed as normalized counts in a regularized logarithm (rlog). Expression levels for off-  
237 target analysis were normalized with those of spike-in controls. A list of genes containing  
238 non-pathological CWG repeats sequences was derived from the spliced RNA in the mouse  
239 reference genome (UCSC GRCm39/mm39). Genes with rlog-transformed expression levels  
240 were processed using DEGreport (version 1.32.0) for clustering analysis and further  
241 processed using clusterProfiler (version 4.4.4) for overrepresentation analysis. Alternative  
242 splicing events were quantified using rMATS (version 4.1.2).

243

## 244 **Electrophysiology**

245 To evaluate neuronal plasticity, hippocampal sections were prepared as previously  
246 described (87). Briefly, the brains were quickly removed from ether-anesthetized mice and  
247 chilled in ice-cold oxygenated artificial cerebrospinal fluid (124 mM NaCl, 5 mM KCl, 26  
248 mM NaHCO<sub>3</sub>, 2 mM CaCl<sub>2</sub>, 2 mM MgSO<sub>4</sub>, 1.25 mM NaH<sub>2</sub>PO<sub>4</sub>, and 10 mM D-glucose).  
249 Sagittal hippocampal slices of 400- $\mu$ m thickness were transferred to a recording chamber,  
250 where they were allowed to recover for at least 1 h at room temperature (24°C to 26°C) before  
251 recording. A concentric bipolar stimulating electrode (FHC, Inc.) was placed in the stratum  
252 radiatum of CA1 to stimulate the Schaffer collateral pathway. An HFS of 100 Hz with a 1-s  
253 duration was applied twice with a 20-s interval. Traces were obtained and analyzed using  
254 SutterPatch version 2.2 (Sutter Instrument).

255

## 256 **AAV preparation**

257 Recombinant AAV9 particles were generated by co-transfection of AAVpro 293T  
258 cells (Takara Bio, Inc.) with three plasmids: pAAV (pAAV-CUG10, pAAV-CUG300,  
259 pAAV-Q23 or pAAV-Q74), pHelper (Stratagene), and pAAV2/9 (kindly provided by Dr. J.  
260 M. Wilson). The viral particles were harvested and purified using AAVpro Purification Kit  
261 Maxi (Takara Bio, Inc.) according to the manufacturer's instructions. Viral titers were  
262 measured using an AAVpro titration kit (Takara Bio, Inc.). For stereotaxic injection of these  
263 viruses into the mouse hippocampus, each virus was diluted to the same titer of  $1.0 \times 10^{13}$   
264 vector genomes/mL.

265

### 266 **Assay for interference with AAV infection**

267 To evaluate the effect of CWG-cPIP on the stability of recombinant AAV, CWG-  
268 cPIP (0.756 nmol) was mixed with purified AAV ( $1.0 \times 10^{10}$  vg) for 3 days at room  
269 temperature. The samples were subjected to SDS-PAGE and AAV capsid proteins VP1, VP2,  
270 and VP3 were visualized by Coomassie Brilliant Blue staining. Images were acquired using  
271 a chemiluminescence imaging system (FUSION SOLO), and the band intensities were  
272 normalized by values of vehicle-treated AAV for each repeat length. Transduction efficiency  
273 was evaluated by AAV infection in HEK293 cells. Twenty-four hours after cell seeding  
274 (20,000 cells/well in 12-well plates), recombinant AAV (multiplicity of infection:  $1 \times 10^5$   
275 vg/cell) and CWG-cPIP (0.756 nmol) were co-treated and cultured for another 3 days. Cells  
276 were fixed, stained with DAPI, and subjected to confocal microscopy (LSM900). GFP-  
277 positive cells were considered as AAV-infected populations.

278

### 279 **Stereotaxic surgery**

280 Male mice were stereotaxically injected with CWG-cPIP and recombinant AAV9 at  
281 nine weeks of age. Under anesthesia, the mice were placed in a stereotaxic instrument  
282 (Narishige), and holes were drilled in the cranium. A mixture of CWG-cPIP (0.5  $\mu$ L, 0.756  
283 nmol) and each AAV9 (1.0  $\mu$ L,  $1.0 \times 10^{13}$  vector genomes/mL) in 1.5% DMSO/PBS per  
284 hemisphere was injected bilaterally into the CA1 region of the dorsal hippocampus using a  
285 26s-gauge needle. Coordinates relative to the bregma were as follows (in mm): anterior, -2.2;  
286 lateral,  $\pm 1.5$ ; ventral, -2.1 for hippocampus; anterior, -0.5; lateral,  $\pm 1.0$ ; ventral, -2.3 for

287 lateral ventricle. Three weeks after the injection, these mice were behaviorally,  
288 electrophysiologically, and immunohistochemically analyzed. To assess tissue distribution  
289 and retention of injected CWG-cPIP, FITC-labeled CWG-cPIP (0.5 $\mu$ L in 1.5 or 10%  
290 DMSO/PBS per hemisphere) was injected at doses of 0.00756, 0.0756, 0.756, or 6.048 nmol  
291 per hemisphere, and immunohistochemical analysis was performed 1, 3, and 7 days later.

292

### 293 **Behavioral analysis**

294 Mice injected with AAVs were subjected to the Y-maze, NOR, PA tests, which were  
295 prepared as previously described (87). In the Y-maze test, spontaneous alternation behavior  
296 in the Y-maze was assessed as a spatial reference memory task. The apparatus consisted of  
297 three identical Plexiglas arms (44  $\times$  13  $\times$  12 cm<sup>3</sup>). Mice were placed at the end of one arm  
298 and were allowed to move freely through the maze during an 8-min session. The sequence  
299 of arm entries was recorded manually. Alternation was defined as entry into all three arms  
300 on consecutive choices. The maximum number of alternations was defined as the total  
301 number of arms entered minus two, and the percentage of alternations was calculated as the  
302 actual alternations/maximum alternations  $\times$  100. The total number of arms entered during  
303 each session was determined. In the NOR test, mice were individually habituated to an open-  
304 field box (28  $\times$  17  $\times$  13 cm<sup>3</sup>) for 2 consecutive days. During the acquisition phase, two objects  
305 of the same material were placed symmetrically at the center of the box for 10 min. Twenty-  
306 four hours later, one object was replaced by a novel object, and exploratory behavior was  
307 analyzed again for 10 min. After each session, the objects were thoroughly cleaned with 70%  
308 ethanol to prevent odor recognition. Exploration of an object was defined as rearing on the

309 object, sniffing it at a distance of < 1 cm, touching it with the nose, or both. Successful  
310 recognition was reflected by preferential exploration of the novel object. The discrimination  
311 of novelty was assessed by comparing the difference between exploratory contacts of novel  
312 and familiar objects and the total number of contacts with both, making it possible to adjust  
313 for differences in total exploration contacts. In the PA test, training and retention trials were  
314 conducted in a box consisting of dark and light compartments ( $13 \times 11 \times 20 \text{ cm}^3$ ). The floor  
315 was constructed with stainless steel rods, and the rods in the dark compartment were  
316 connected to an electronic stimulator (Med Associates, Inc.). Mice were habituated to the  
317 apparatus for 2 days prior to passive avoidance acquisition. During training, a mouse was  
318 placed in the light compartment, and on entering the dark compartment, the door was closed  
319 and an electric shock (0.5 mA for 3 s) was delivered from the floor. The mouse was removed  
320 from the apparatus 30 s later. The next day, each mouse was placed in the light compartment,  
321 and step-through latency was recorded for over 300 s to assess retention. The videotapes for  
322 all behavioral analyses were scored by a trained observer blinded to the drug treatment.

323         Motor function in R6/2 mice were assessed by rotarod and hind-limb clasping tests  
324 as previously described (91). In the rotarod test, mice were placed on a stationary rod (30  
325 mm diameter; Muromachi Kikai) and left in place for 60 s. The mice were then forced to  
326 walk on the accelerating rods (4–40 rpm) for up to 300 s. An hour later, the mice were  
327 subjected to the second trial, and the latency to fall was measured for each trial. In the hind-  
328 limb clasping test, mice were suspended by their tails for 30 s at a height of 50 cm from the  
329 home-cage and hindlimb clasping was scored as follows: score 0, hind-limbs consistently  
330 stretched outward from the abdomen; score 1, hind-limbs individually, but not both at the

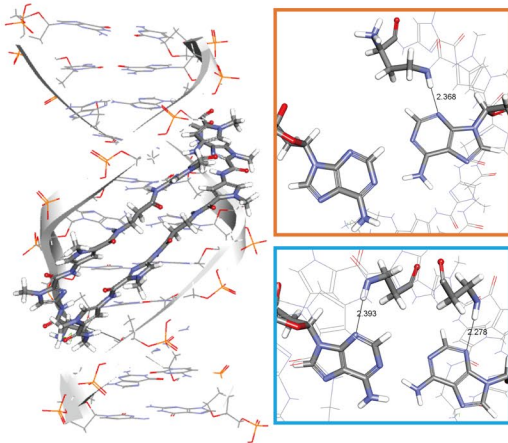
331 same time, retract toward the abdomen with a cumulative time less than 15 s; score 2, hind-  
332 limbs individually, but not both at the same time, retract toward the abdomen with a  
333 cumulative time 15 s or more; score 3, both hind-limbs retract toward and touch the abdomen  
334 at the same time.

335 **Supplementary Figures**

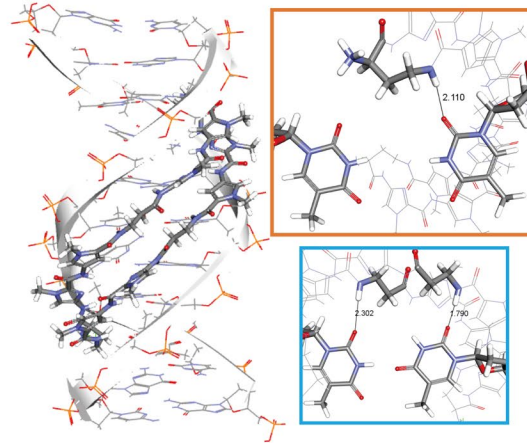
**A**

	N = A	N = T	N = G	N = C
NH ( $\gamma$ -turn) - N (Å)	2.3 ± 0.04	2.0 ± 0.1	4.7 ± 0.4	2.5 ± 0.8
NH ( $\beta$ -alanine) - N (Å)	2.3 ± 0.1	2.0 ± 0.4	3.4 ± 0.9	1.9 ± 0.02

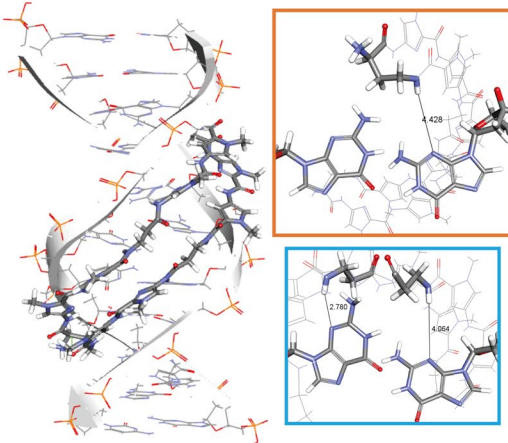
**B** N = A



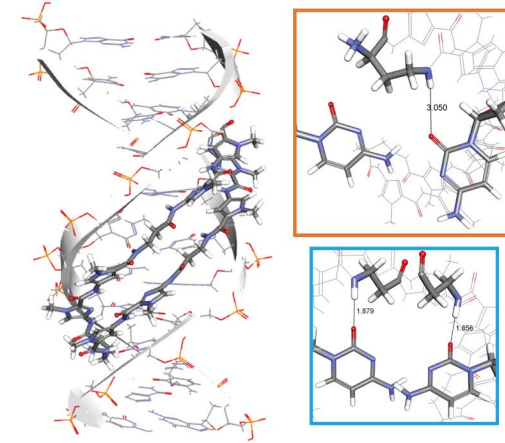
**C** N = T



**D** N = G



**E** N = C



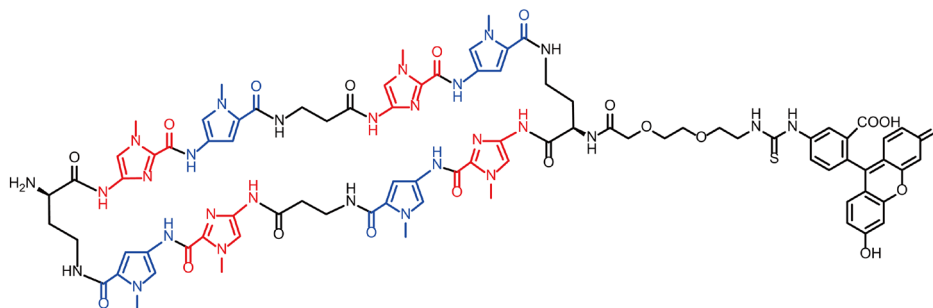
336

337

338 **Supplementary Figure 1. Binding modes of CWG-cPIP for CNG repeat DNA.**

339 **(A)** The interaction distances of hydrogen bonds between DNA base pairs (N: A, T, G, or C)  
340 and  $\gamma$ -turn (orange) or  $\beta$ -alanine (blue) in CWG-cPIP. For description of a schematic  
341 illustration of DNA sequence recognition by CWG-cPIP, see Figure 1A. **(B–E)** Molecular  
342 models of CWG-cPIP/double-stranded CAG- (B), CTG- (C), CGG- (D), or CCG- (E) DNA  
343 complex by computer-assisted molecular simulation. Data represent mean  $\pm$  SEM.

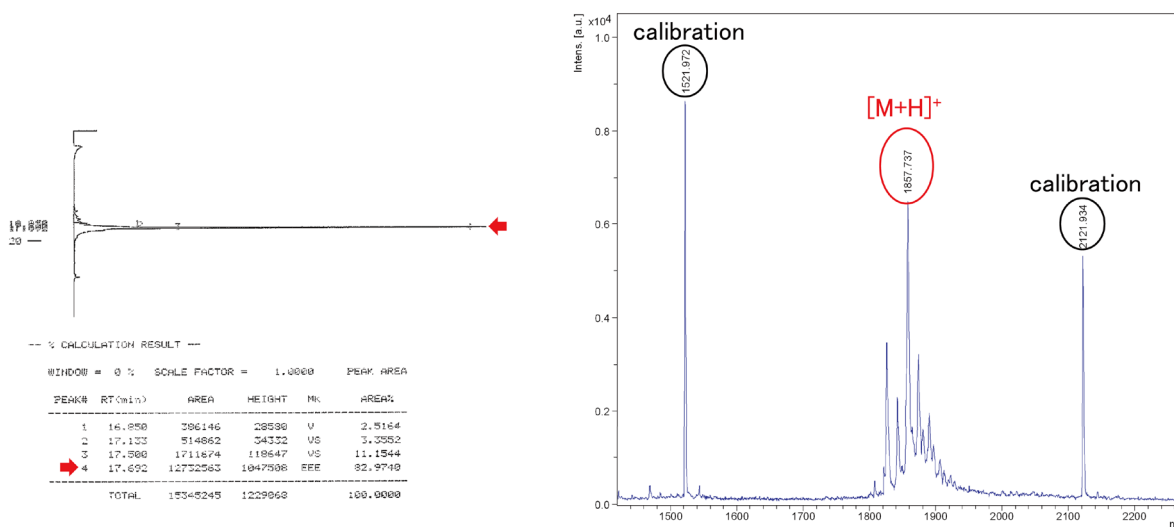
## FITC-labeled CWG-cPIP



Chemical Formula:  $C_{85}H_{92}N_{28}O_{20}S$

Exact Mass: 1856.68

Molecular Weight: 1857.91

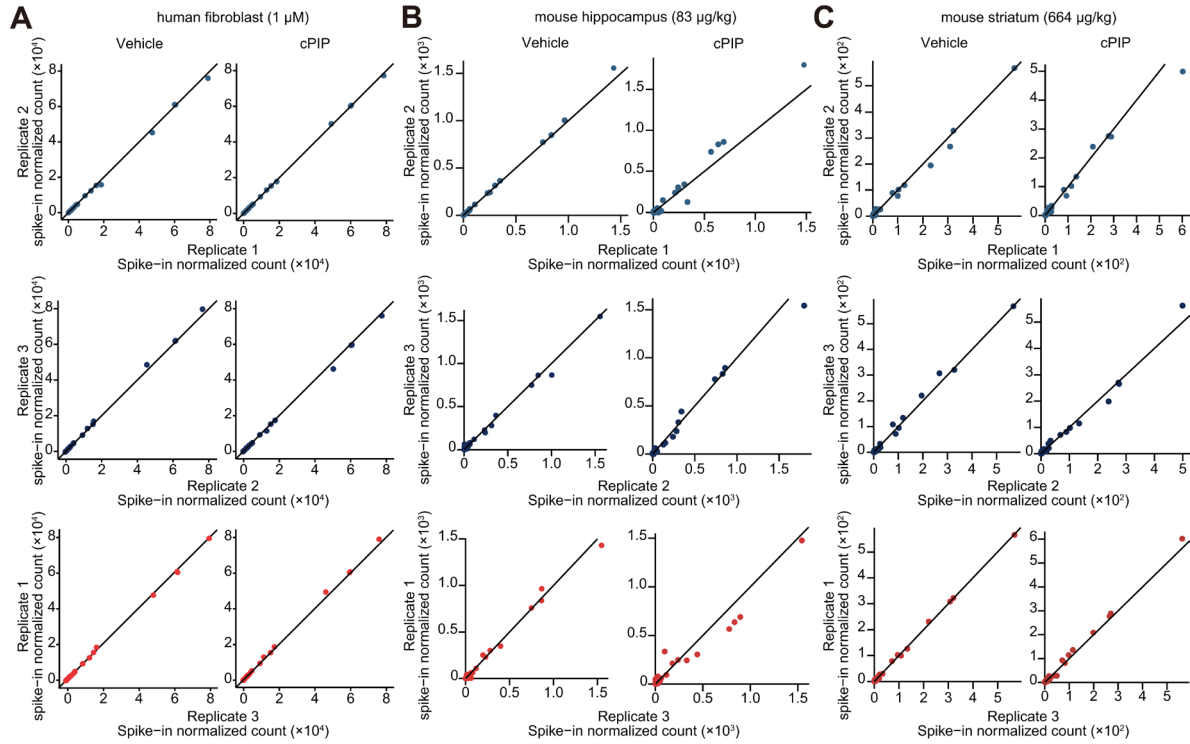


344

### 345 **Supplementary Figure 2. Synthesis of FITC-labeled CWG-cPIP.**

346 (top) Chemical structure of FITC-labeled CWG-cPIP. (bottom) HPLC and MALDI-TOF MS  
 347 spectra of FITC-labeled CWG-cPIP. Conditions: equilibrated with 0.1% trifluoroacetic acid  
 348 with a linear gradient from 0% to 100% acetonitrile at a flow rate of 1.0 mL/min for 40 min,  
 349 detected at 254 nm. Arrows indicate the peak and the retention time (17.692 min). m/z found;  
 350 1857.737.

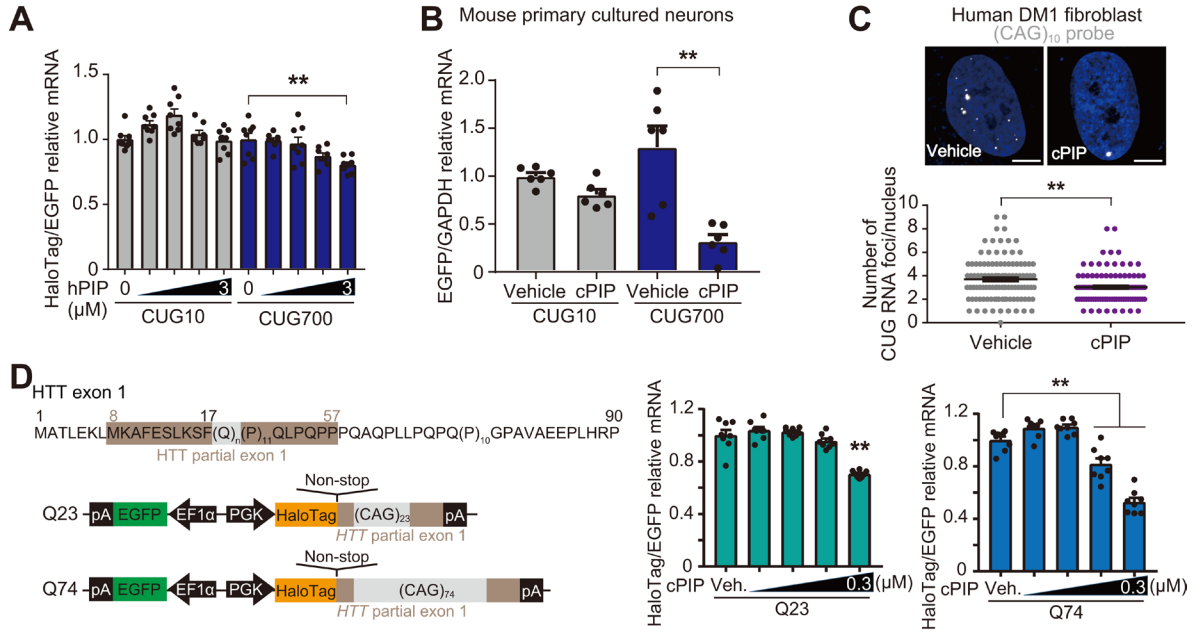
351



352

353 **Supplementary Figure 3. Abundances of spike-in controls in RNA-seq analyses.**

354 (A–C) Comparisons of transcripts with normalized count of spike-in controls between  
 355 replicates in RNA-seq analyses using human fibroblasts treated with 1 $\mu$ M CWG-cPIP (A),  
 356 mouse hippocampus with 83  $\mu$ g/kg CWG-cPIP (B), and mouse striatum with 664  $\mu$ g/kg  
 357 CWG-cPIP (C).

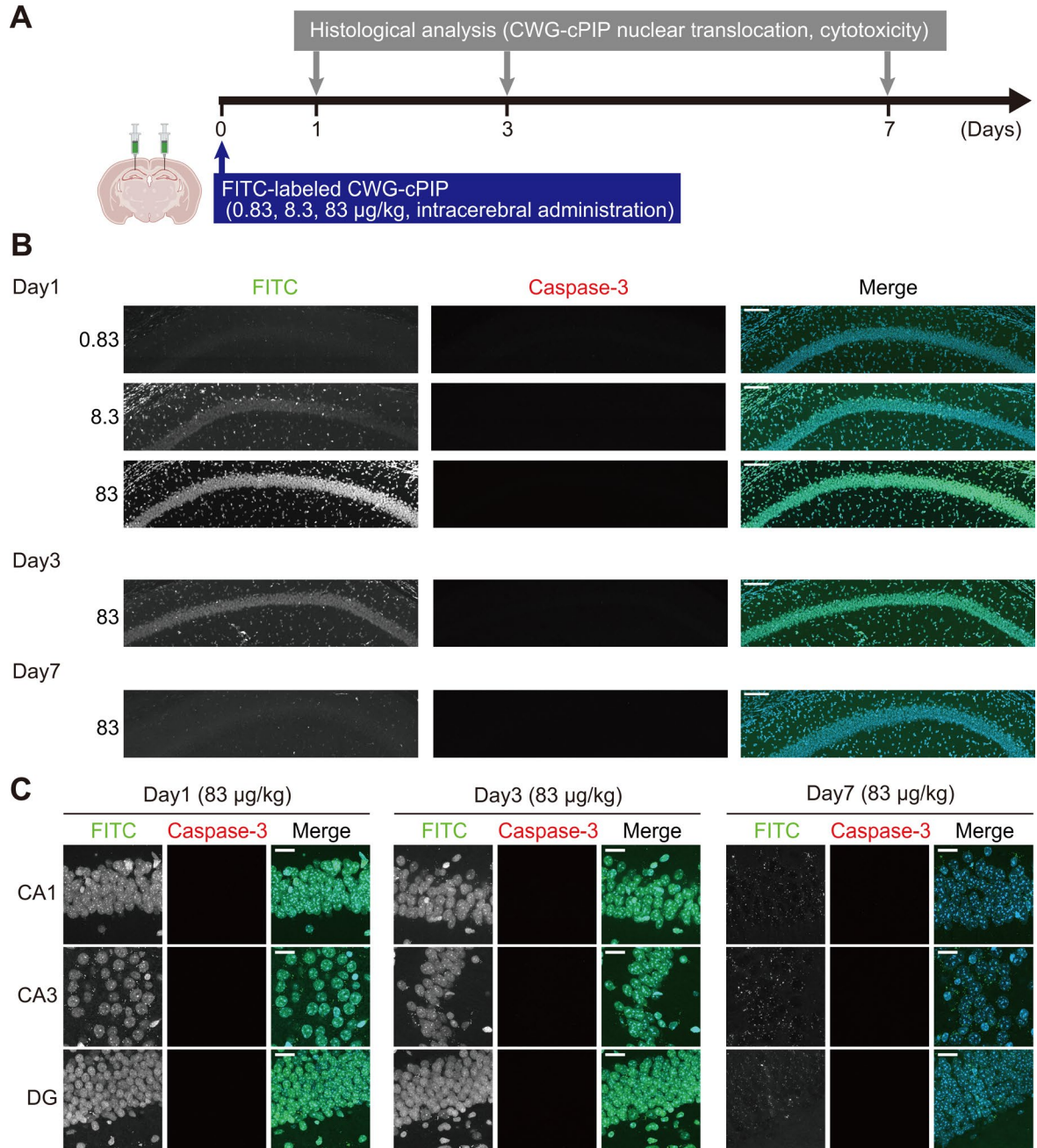


358

359 **Supplementary Figure 4. Inhibition of transcription and pathogenic CUG RNA in**  
 360 **CWG repeat-expanded cell models by CWG-cPIP treatment.**

361 **(A)** Quantification of HaloTag mRNA levels in Neuro-2a cells treated with CWG-hPIP at  
 362 concentrations of 0.1, 0.3, 1, and 3 μM. **\*\*** $P < 0.01$  by one-way ANOVA with Bonferroni's  
 363 multiple comparisons test.  $n = 8$  each. **(B)** Quantification of *Egfp* mRNA levels in mouse  
 364 primary neurons treated with 1 μM CWG-cPIP. **\*\*** $P < 0.01$  by two-way ANOVA with  
 365 Bonferroni's multiple comparisons test.  $n = 6$  each. **(C)** Representative confocal images of  
 366 CUG-RNA foci (white) in DM1 patient-derived fibroblasts (top). Scale bars, 5 μm;  
 367 quantification of CUG-RNA foci (bottom). **\*\*** $P < 0.01$  by two-sided unpaired Student's *t*-  
 368 test. Vehicle:  $n = 108$  cells; CWG-cPIP:  $n = 100$  cells. **(D)** Amino acid sequences of human  
 369 HTT exon 1 (left, top). Residue numbers refer to HTT with Q23 repeat. Schematic  
 370 representation of constructs with CAG repeat sequences in a coding region used for RT-  
 371 qPCR in Neuro-2a cells (left, bottom); quantification of HaloTag mRNA levels (right).

372 CWG-cPIP concentrations were 0.01, 0.03, 0.1, and 0.3  $\mu\text{M}$ .  $**P < 0.01$  by one-way ANOVA  
373 with Bonferroni's multiple comparisons test.  $n = 8$  each. Data represent mean  $\pm$  SEM. Source  
374 data are provided in Supplementary File 6.

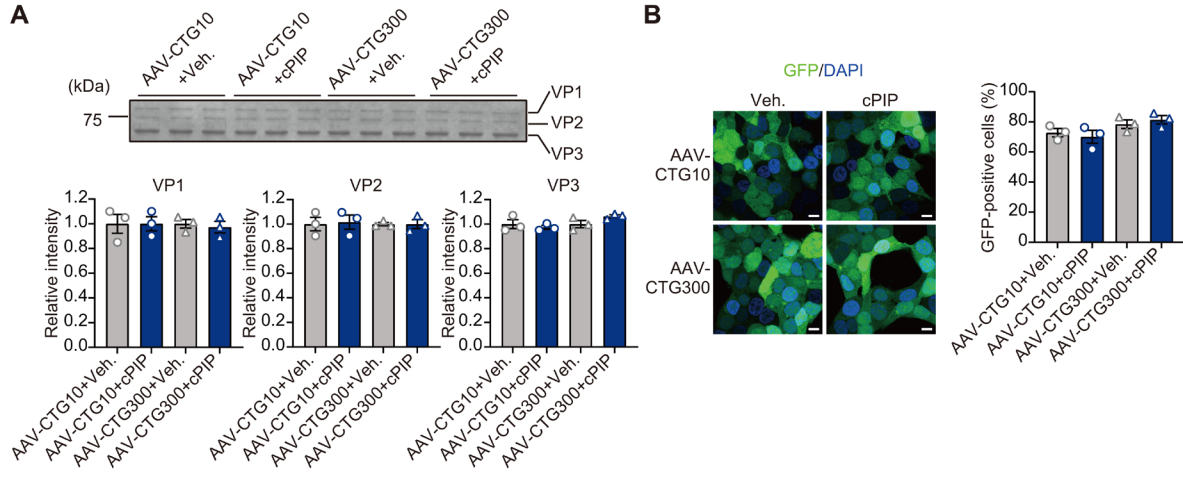


375

376 **Supplementary Figure 5. Nuclear penetration of CWG-cPIP without cell toxicity after**  
 377 **intracerebral injection.**

378 **(A)** Experimental diagram of intracerebral injection of FITC-labeled CWG-cPIP into intact  
 379 mice and the immunohistochemical analysis. **(B, C)** Representative confocal images of

380 FITC-labeled CWG-cPIP and cleaved caspase-3 in the hippocampal CA1, CA3, and DG  
381 subregions. Scale bars, 100  $\mu\text{m}$  (B) and 20  $\mu\text{m}$  (C).



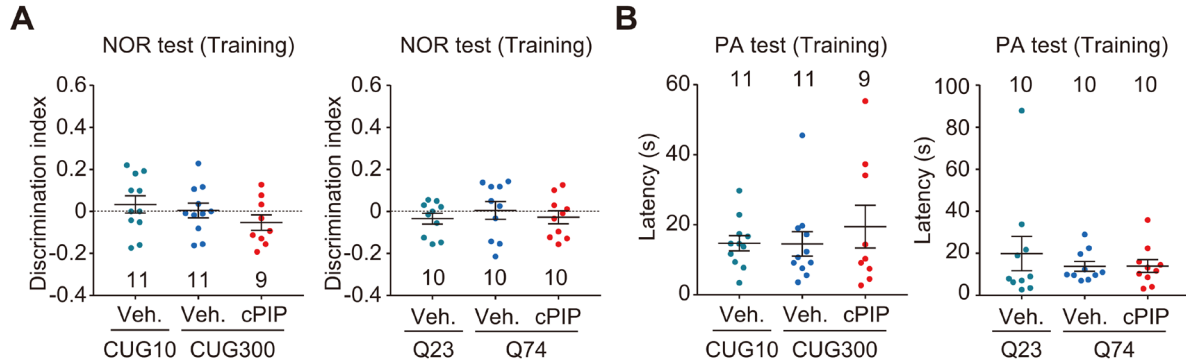
382

383 **Supplementary Figure 6. No interference of CWG-cPIP on recombinant AAV.**

384 **(A)** Gel images stained with Coomassie Brilliant Blue after treatment of recombinant AAV  
 385 with CWG-cPIP in vitro (top) and quantifications of the band intensities (bottom). n = 3 each.

386 Statistics were performed by two-sided unpaired Student's t-test. **(B)** Representative images  
 387 of GFP-positive HEK293 cells co-treated with recombinant AAV and CWG-cPIP (left) and  
 388 quantification of GFP-positive cells (right). n = 3 each, acquired from 3 images in each  
 389 experiment. Statistics were performed by two-sided unpaired Student's t-test. Data represent

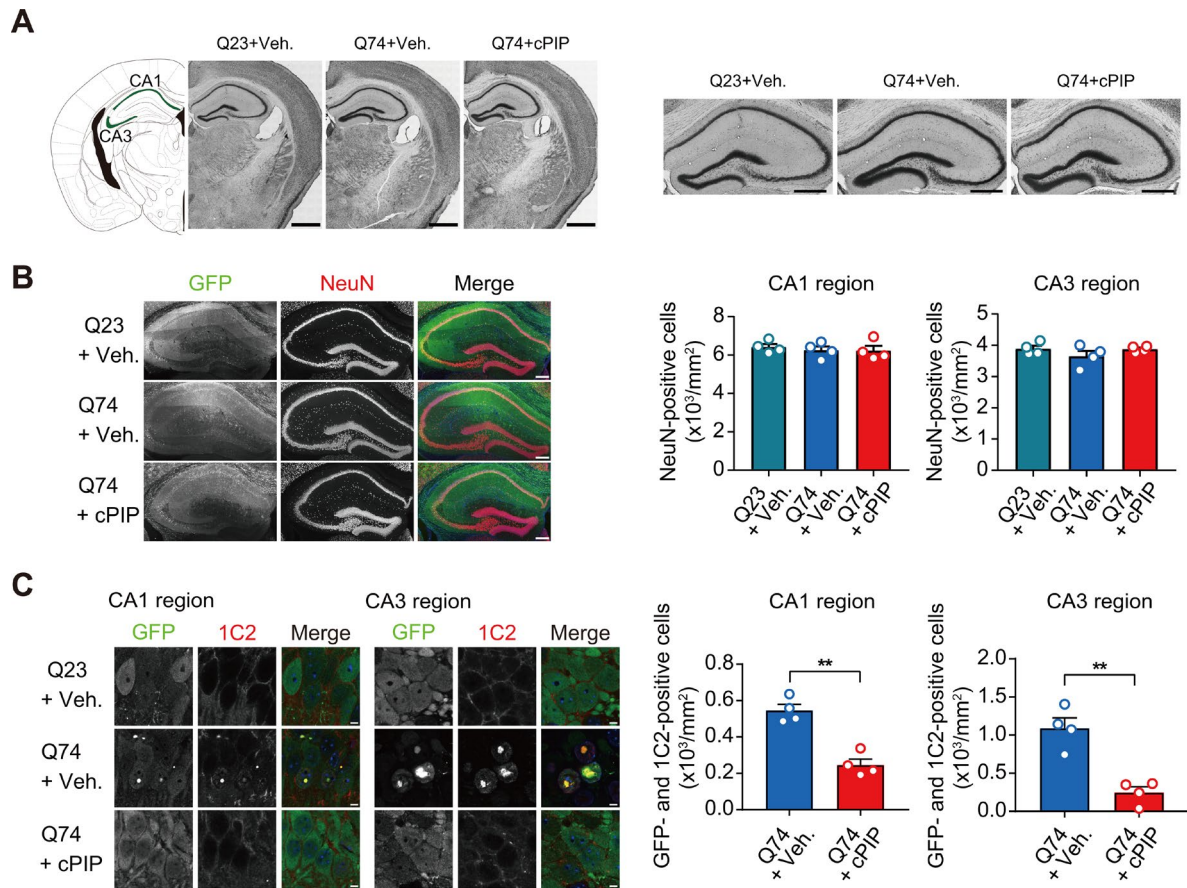
390 mean ± SEM. Source data are provided in Supplementary File 6.



391

392 **Supplementary Figure 7. Normal behaviors of mice in training sessions of memory-**  
 393 **related tests.**

394 **(A)** Discrimination indices in the training sessions of the NOR test. Statistics were performed  
 395 by one-way ANOVA with Bonferroni's multiple comparisons test. CUG10 + vehicle and  
 396 CUG300 + vehicle:  $n = 11$  mice; CUG300 + CWG-cPIP:  $n = 9$  mice (left);  $n = 10$  mice each  
 397 (right). **(B)** Latency to enter the dark compartment in the training sessions of the PA test.  
 398 Statistics were performed by one-way ANOVA with Bonferroni's multiple comparisons test.  
 399 CUG10 + vehicle and CUG300 + vehicle:  $n = 11$  mice; CUG300 + CWG-cPIP:  $n = 9$  mice  
 400 (left);  $n = 10$  mice each (right). Data represent mean  $\pm$  SEM. Source data are provided in  
 401 Supplementary File 6.

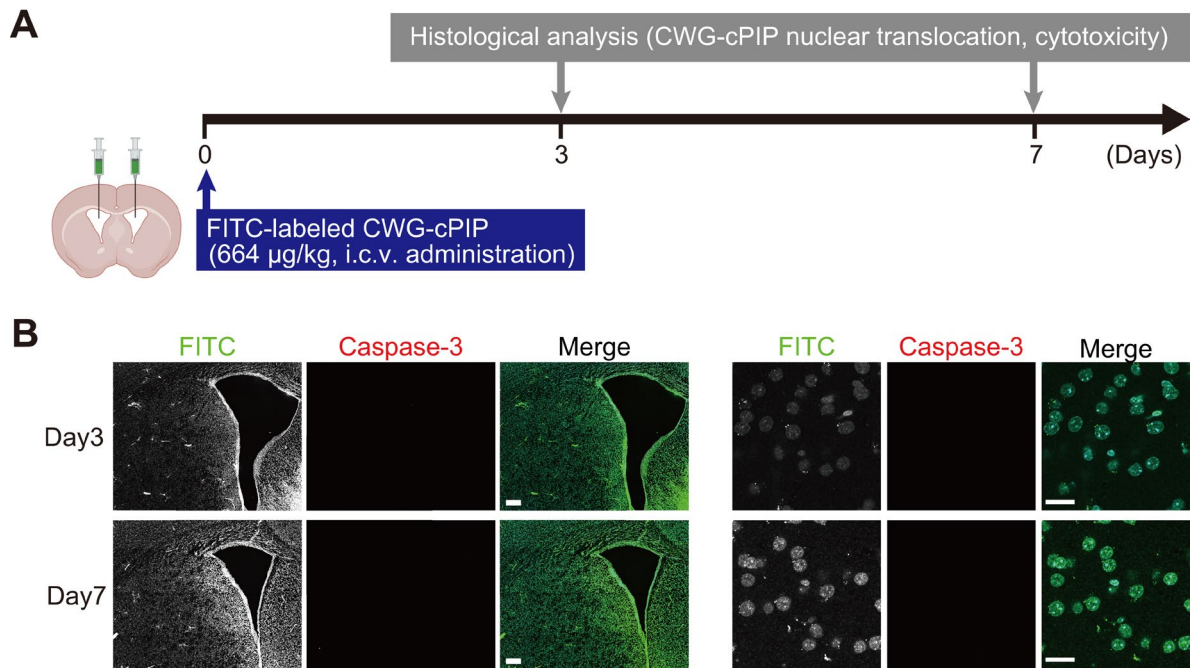


402

403 **Supplementary Figure 8. Inhibition of polyQ aggregation seen in a CAG repeat-**  
 404 **expanded mouse model by CWG-cPIP treatment.**

405 **(A)** Representative confocal images of Nissl-stained sections. Scale bars, 1 mm (left) and  
 406 500  $\mu\text{m}$  (right). **(B)** Representative confocal images of GFP (green) and NeuN (red) in the  
 407 hippocampus (left) and the quantification of NeuN-positive cells in CA1 and CA3 regions  
 408 (right). Statistics were performed by one-way ANOVA with Bonferroni's multiple  
 409 comparisons test.  $n = 4$  mice each, averaged from three independent replicates (three slices)  
 410 per mouse. Scale bars, 200  $\mu\text{m}$ . **(C)** Representative confocal images of polyQ aggregates in  
 411 the hippocampal CA1 and CA3 regions (left) and their quantification (right).  $**P < 0.01$  by  
 412 two-sided unpaired Student's t-test.  $n = 4$  mice each, averaged from three independent

413 replicates (three slices) per mouse. Scale bars, 5  $\mu\text{m}$ . Data represent mean  $\pm$  SEM. Source  
414 data are provided in Supplementary File 6.



416

417 **Supplementary Figure 9. Nuclear penetration of CWG-cPIP without cell toxicity after**  
 418 **i.c.v. injection.**

419 **(A)** Experimental diagram of i.c.v. injection of FITC-labeled CWG-cPIP into intact mice and  
 420 the immunohistochemical analysis. **(B, C)** Representative confocal images of FITC-labeled  
 421 CWG-cPIP and cleaved caspase-3 in the striatum. Scale bars, 200 µm (B) and 20 µm (C).

	double-stranded DNA				1bp mismatched hairpin DNA				1bp mismatched hairpin RNA	
										
	d(CAG/CTG)	d(CCG/CGG)	AT rich	GC rich	d(CAG) <sub>10</sub>	d(CTG) <sub>10</sub>	d(CGG) <sub>10</sub>	d(CCG) <sub>10</sub>	r(CUG) <sub>10</sub>	r(CAG) <sub>10</sub>
$T_m$ (°C) (vehicle)	43.4 ± 0.1	57.6 ± 0.9	28.4 ± 3.6	79.1	49.9 ± 0.3	50.7 ± 0.1	66.8 ± 0.6	48.3 ± 0.1	47.8 ± 0.2	59.7 ± 0.5
$\Delta T_m$ (hPIP-vehicle)	38.8 ± 0.8	17.1 ± 2.4	10.8 ± 0.5	-11.6 ± 2.9	36.2 ± 0.05	34.5 ± 0.3	3.24 ± 0.6	31.1 ± 1.7	-0.13 ± 1.7	-2.70 ± 0.6
$\Delta T_m$ (cPIP-vehicle)	51.6 ± 0	14.5 ± 0.4	2.24 ± 0.04	-1.22 ± 1.3	45.1 ± 0	41.4 ± 0.4	3.64 ± 0.3	30.3 ± 0.6	-0.14 ± 0.1	-2.27 ± 0.2

422

423 **Supplementary Table 1.  $T_m$  and  $\Delta T_m$  in the melting temperature assay for indicated**

424 **DNAs and RNAs with PIPs addition.**

425 **References**

- 426 87. Shioda N, et al. Targeting G-quadruplex DNA as cognitive function therapy for ATR-X  
427 syndrome. *Nat. Med.* 2018;24(6):802–813.
- 428 88. Hu W, et al. Direct Conversion of Normal and Alzheimer's Disease Human Fibroblasts  
429 into Neuronal Cells by Small Molecules. *Cell Stem Cell* 2015;17(2):204–212.
- 430 89. Yang J, et al. Small molecular compounds efficiently convert human fibroblasts directly  
431 into neurons. *Mol. Med. Rep.* 2020;22(6):4763–4771.
- 432 90. Osmand AP, et al. Imaging Polyglutamine Deposits in Brain Tissue. *Methods Enzymol.*  
433 2006;412:106–122.
- 434 91. Kumar MJV et al. Spatiotemporal analysis of soluble aggregates and autophagy markers  
435 in the R6/2 mouse model. *Sci. Rep.* 2021;11(1):96.